scientific reports

Check for updates

OPEN

Clinical and neuroimaging correlates of disease related gait patterns in patients with multiple system atrophy cerebellar type

Seungmin Lee[1,8], Minchul Kim[2,8], Kyu Sung Choi[3,7,8], Chanhee Jeong[1], Ri Yu[4], Jee-Young Lee[5], Jung Hwan Shin[1]✉, Han-Joon Kim[1]✉ & Beomseok Jeon[6]

Multiple system atrophy-cerebellar type (MSA-C) is a rapidly progressive neurodegenerative disorder, yet objective digital biomarkers for disease severity remain scarce. This cross-sectional study aimed to identify disease-relevant gait patterns using a 2D video-based gait analysis algorithm and examine their clinical and neuroimaging correlates. Gait features were extracted from videos of patients with MSA-C using *Gaitome*, and an MSA-C gait pattern score was derived. This score significantly distinguished MSA-C from healthy controls (area under the curve = 0.98) and showed significant correlations with UMSAR part I ($r = 0.49$, $p = 0.0014$), part II ($r = 0.51$, $p = 0.0014$), MMSE ($r = -0.43$, $p = 0.012$), and MoCA ($r = -0.34$, $p = 0.049$). Tractography revealed significant associations between the gait score and structural connectivity in the middle cerebellar peduncle, cerebellum, and cingulate. Voxel-based morphometry showed that the gait score correlated with gray matter volume in the middle temporal and cerebellar regions, whereas UMSAR part II did not show significant structural associations. These findings suggest that gait patterns extracted from a single video camera can reflect both motor and cognitive severity in MSA-C, and may serve as a practical, non-invasive digital biomarker for disease monitoring.

Keywords MSA-C gait pattern score, Video-based analysis, DTI, VBM

Multiple system atrophy (MSA) is a neurodegenerative disease characterized by cerebellar ataxia, parkinsonism, and autonomic dysfunction[1]. Patients with MSA experience rapid disease progression, impaired balance, and frequent falls. Within an average of three years, up to 30% of patients require a walking aid, and within an average of five years, up to 60% require the use of a wheelchair[2]. The median survival is reported to be approximately six–ten years, reflecting a poor prognosis[3–5], with no disease-modifying therapy proven effective[6]. Given the rapid progression of the disease, objective and reliable evaluation methods are essential for clinical monitoring and assessment of outcomes in clinical trials.

The Unified Multiple System Atrophy Rating (UMSAR) score is widely used to assess disease severity and progression in MSA[7,8]. However, there may be certain considerations, such as reduced applicability in advanced stages and variability depending on the rater[9,10]. Although UMSAR score encompasses key symptom categories, including parkinsonism, cerebellar ataxia, and autonomic dysfunction, it may not fully capture the distinct clinical profiles of the of cerebellar (MSA-C) and parkinsonian (MSA-P) subtypes, especially during early disease stages[8]. Notably, patients with MSA-C often suffer from greater postural instability and have higher Hoehn and Yahr stages, which reflect more advanced motor disability and dependency, compared to MSA-P, despite similar disease duration[1]. They also reach critical disability milestones, such as falls, urinary incontinence,

[1]Department of Neurology, Seoul National University Hospital, Seoul National University College of Medicine, 101 Daehak-ro, Jongno-gu, Seoul 03080, South Korea. [2]Department of Radiology, Kangbuk Samsung Hospital, Sungkyunkwan University School of Medicine, Seoul, South Korea. [3]Department of Radiology, Seoul National University Hospital, Seoul National University College of Medicine, Seoul National University, Seoul, South Korea. [4]Department of Software and Computer Engineering, Ajou University, Suwon, South Korea. [5]Department of Neurology, Seoul Metropolitan Government-Seoul National University Boramae Medical Center, Seoul National University College of Medicine, Seoul, South Korea. [6]Department of Neurology, Chung-ang University Health Care System Hyundae Hospital, Namyangju, South Korea. [7]Healthcare AI Research Institute, Seoul National University Hospital, Seoul, South Korea. [8]Seungmin Lee, Minchul Kim and Kyu Sung Choi contributed equally to this work. ✉email: neo2003@snu.ac.kr; movement@snu.ac.kr

and wheelchair dependence earlier than their MSA-P counterparts[11]. These differences highlight the need for objective tools to monitor axial motor symptoms, particularly gait and balance, in patients with MSA-C during early stages of the disease.

With the advancements in computer vision technologies, a growing number of studies have utilized video-based approaches to assess the clinical severity of movement disorders[12]. Several studies have successfully demonstrated the feasibility of quantifying individual motor features such as facial bradykinesia[13], pose-estimation[14], and video-based prediction of Parkinson's disease (PD) motor severity[15]. Our work extends this approach by integrating them into a unified and interpretable metric. We have previously published algorithms that can capture the motor features of posture, locomotion, and turning gait parameters[14,16,17]. These components represent core motor domains that can be evaluated during simple gait assessments using standard video recordings.

Thus, in this study, we aimed to derive comprehensive motor-related patterns from gait videos of patients with MSA-C, investigate their role as potential biomarkers by assessing clinical correlations and demonstrate how these patterns reflect the pathophysiology of MSA-C through structural and connectivity analyses using brain imaging.

Results

Patient characteristics

During the study period, 42 patients with MSA-C and 27 HCs were enrolled (Table 1). To derive the disease-specific gait pattern, we selected a subgroup of 30 patients with MSA-C and 27 HCs in which the p-value for sex was the highest, and the sum of the p-values for age, sex, and height was also maximized (Table S1). This matched subgroup was used to define the MSA-C gait pattern, which was subsequently applied to the full MSA-C cohort ($n = 42$) to compute individual gait pattern scores.

Overall, the MSA-C cohort had a higher proportion of male participants compared to the HC group. MMSE scores were not significantly different between the groups, with the mean disease duration in the MSA-C cohort at time of study enrollment was 1.8 ± 1.0 years (Table 1). Disease duration showed a positive correlation with UMSAR part II scores ($r = 0.33$, uncorrected $p = 0.031$); however, this correlation did not remain significant after FDR correction. (Figure S1). Both MMSE and MoCA scores showed significant negative correlations with disease duration (MMSE: $r = -0.36$, $p = 0.041$; MoCA: $r = -0.33$, $p = 0.041$) (Figure S2).

MSA-C gait pattern scores and clinical correlation: *Gaitome*-derived score

A covariance matrix of gait parameters from the age-matched MSA-C and HCs was calculated, followed by principal component analysis (PCA) (Fig. 1d). The first five principal components (PCs) accounted for 83.8% of the total variance in the spatial map of gait parameters. A combination of PCs 1 through 4 yielded the best discrimination between patients with MSA-C and HCs (AUC = 0.98; Fig. 1d) with a sensitivity of 0.90 and a specificity of 0.93. Their spatial weights were defined as the MSA-C gait pattern.

Among the 18 gait parameters, the MSA-C gait pattern was positively correlated with step width, turning time, and turning step number (z-score > 1), and negatively correlated with step length, velocity, and turning velocity (z-score < -1) (Fig. 1e). Parameters showing significant differences, including step length, step length variability, step width, velocity, step length asymmetry, turning time, turning step number, turning velocity, and dropped head angle, were identified as key contributors to the MSA-C gait pattern. (Figure S3). We confirmed that the parameters representing the gait pattern of MSA-C were stable with bootstrapping resampling (Figure S4). Gait pattern scores were significantly higher in the MSA-C group compared to the HCs group (Fig. 1f).

MSA-C gait pattern scores and clinical correlation: motor aspect

MSA-C gait pattern scores were significantly correlated with UMSAR part I ($r = 0.49$, $p = 0.0014$) and part II ($r = 0.51$, $p = 0.0014$) scores, adjusted for age, sex, and disease duration (Fig. 2a, b). While all UMSAR part I sub-scores showed a positive trend with MSA-C gait pattern scores, none remained significant after correction for multiple comparisons (Fig. 2c).

	MSA-C ($n = 42$)	HCs ($n = 27$)	p-value
Age at enroll (years)	62.2 ± 8.5	66.0 ± 8.1	0.067
Height (cm)	165.2 ± 8.0	162.2 ± 8.9	0.15
*M: F	28:14	9:18	0.014
Disease duration (years)	1.8 ± 1.0	–	–
MMSE ($n = 40$)	27.2 ± 1.7	27.5 ± 1.8 ($n = 21$)	0.74
MoCA ($n = 40$)	23.9 ± 3.4	–	–
UMSAR part I score	12.6 ± 5.0	–	–
UMSAR part II score	13.2 ± 6.2	–	–
**MSA-C gait pattern (Z-score)	3.8 ± 1.9	0.0 ± 1.0	4.3×10^{-16}

Table 1. Demographic and clinical characteristics of the participants. Data are presented as mean ± standard deviation. *HCs* healthy controls, *F* Female, *M* Male, *MMSE* Mini-Mental State Examination, *MoCA* Montreal Cognitive Assessment, *MSA-C* Multiple System Atrophy-Cerebellar type, *UMSAR* Unified Multiple System Atrophy Rating. *$p < 0.05$, Chi-squared test; **$p < 0.05$, t-test.

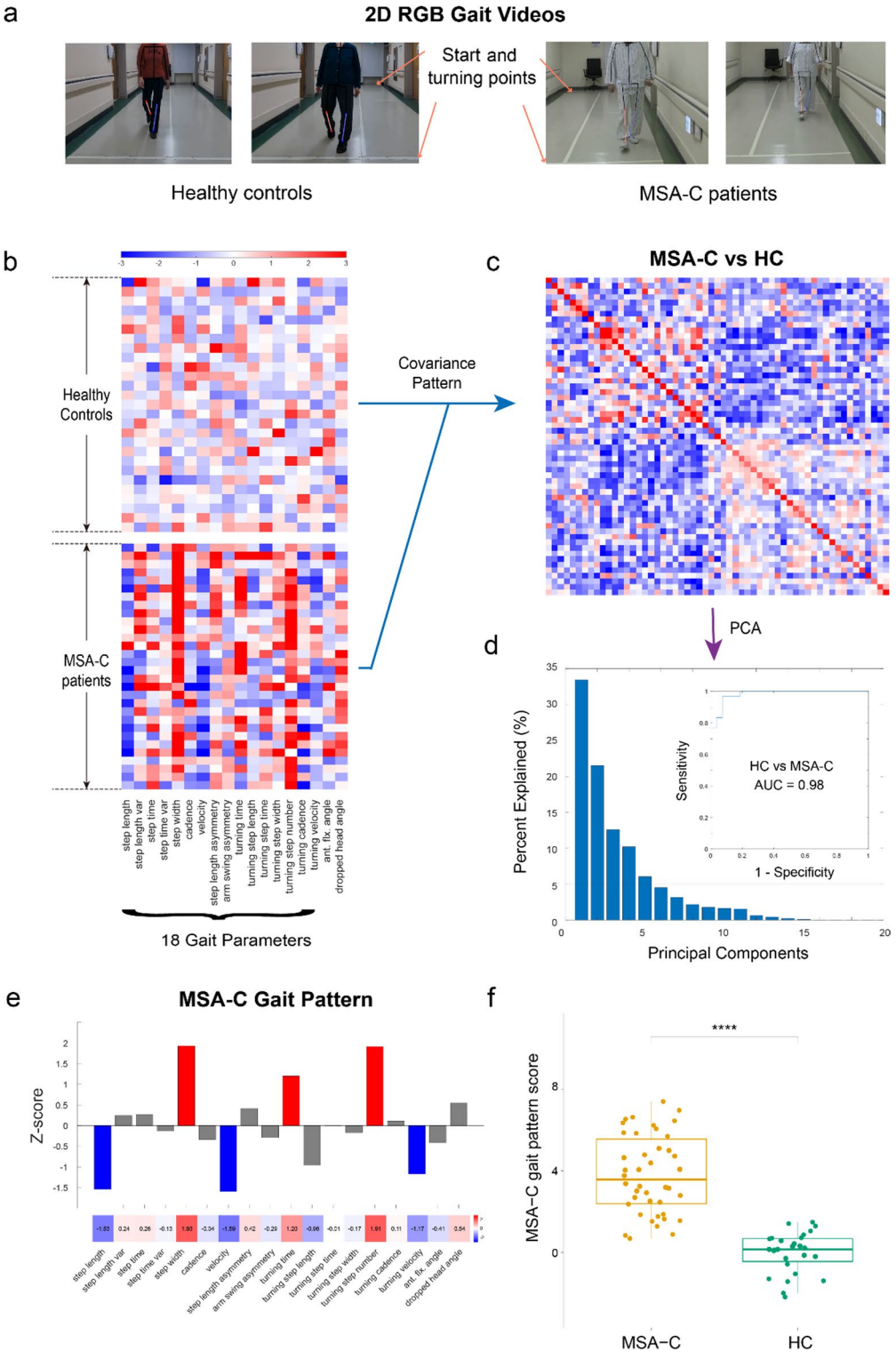

Fig. 1. Schematic diagram for derivation of the MSA-C gait pattern score using the Gaitome algorithm. (**a**) Floor markers indicating the start and turning points for gait tasks, (**b**) Construction of a shared covariance structure from 18 gait parameters of MSA-C patients and HCs, (**c**) Visualization of the shared covariance structure underlying gait features, (**d**) Classification performance using principal components 1–4, (**e**) Gait parameters contributing positively or negatively to the MSA-C gait pattern score, (**f**) Comparison of gait pattern scores between patients with MSA-C and HC. Units: degree—anterior flexion angle, dropped head angle; meter—step length (mean), turning step length (mean), turning step width (mean); meter/second—velocity; second—step time (mean), turning step time (mean); steps per minute—cadence, turning cadence. *AUC* area under the curve, *HC* healthy controls, MSA-C, multiple system atrophy cerebellar type, *PCA* Principal Component Analysis.

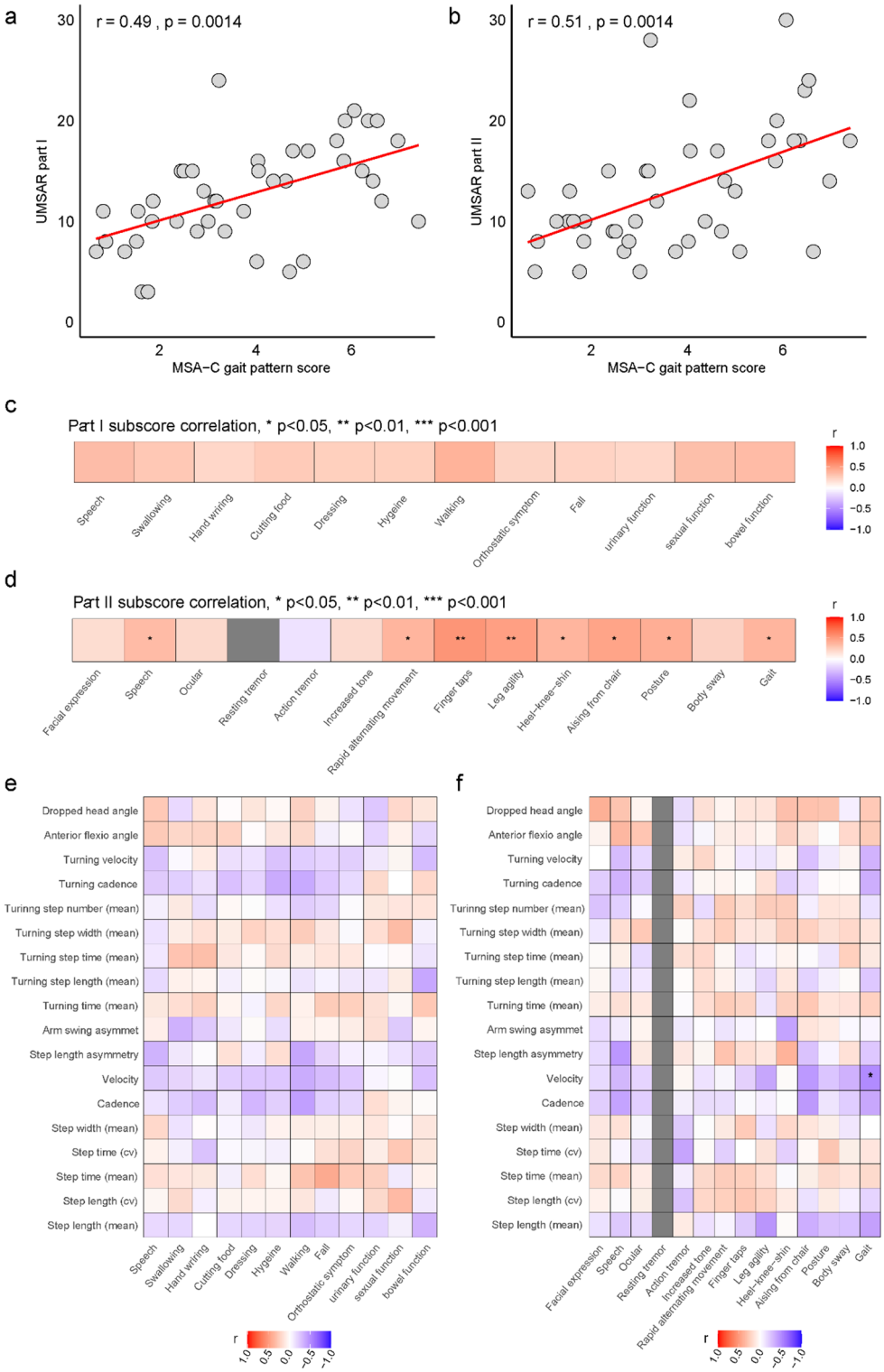

Fig. 2. Correlation matrix between the MSA-C gait pattern score and UMSAR score, UMSAR sub-items, and 18 gait parameters. Scatter plots illustrate the relationships MSA-C gait pattern score with (**a**) UMSAR part I, (**b**) UMSAR part II, (**c**) UMSAR part I subscores, and (**d**) UMSAR part II subscores. Correlation matrix between (**e**) UMSAR part I subscores and gait parameters, and (**f**) UMSAR part II subscores and gait parameters. In each cell, colors indicate the strength of the Spearman partial correlation coefficients, adjusted for age, sex, and disease duration. Statistical significance was denoted with an asterisk (*). $^{*}p<0.05$, $^{**}p<0.01$, $^{***}p<0.001$. Units: degree—anterior flexion angle, dropped head angle; meter—step length (mean), turning step length (mean), turning step width (mean); meter/second—velocity; second—step time (mean), turning step time (mean); steps per minute—cadence, turning cadence. *CV* coefficient of variation, *MSA-C* multiple system atrophy cerebellar type.

In UMSAR part II, the following items were significantly correlated with MSA-C gait pattern scores: speech ($r = 0.33$, $p = 0.039$), rapid alternating movement ($r = 0.37$, $p = 0.020$), finger taps ($r = 0.54$, $p = 0.00042$), leg agility ($r = 0.49$, $p = 0.0017$), heel to shin ($r = 0.37$, $p = 0.019$), arising from chair ($r = 0.47$, $p = 0.0025$), posture ($r = 0.41$, $p = 0.0097$), and gait ($r = 0.37$, $p = 0.020$) (Fig. 2d).

The correlation analysis between individual UMSAR part I sub-items and 18 gait parameters revealed that gait velocity, cadence, step length asymmetry, and turning cadence trended to be negatively correlated with the UMSAR part I walking sub-score (uncorrected $p < 0.05$), while mean step time showed a positive trend with the UMSAR part I falling sub-score (uncorrected $p < 0.05$; Table S2). However, none of these correlations remained significant after correction for multiple comparisons (Fig. 2e, Table S2).

For UMSAR part II, mean step length, gait velocity, dropped head angle, cadence, turning cadence, and turning velocity tended showed negative trends with the gait sub-score (uncorrected $p < 0.05$, Table S3). Mean step length, gait velocity, and cadence showed a correlation with arising from chair sub-score, while gait velocity was negatively associated with body sway sub-score (uncorrected $p < 0.05$; Table S3). Only the correlation between gait velocity and the UMSAR part II gait sub-score remained significant after multiple comparison correction (Fig. 2f, Table S3).

MSA-C gait pattern scores and clinical correlation: non-motor aspect

We next examined non-motor correlates of gait in MSA-C, focusing on cognitive and autonomic function domains. In cognitive aspect, both MMSE and MoCA scores showed a significant negative correlation (MMSE: $r = -0.40$, $p = 0.038$; MoCA: $r = -0.36$, $p = 0.031$) (Fig. 3a, b). Among UMSAR scores, only part II was significantly correlated with MMSE scores (part I: $r = -0.27$, $p = 0.16$; part II: $r = -0.45$, $p = 0.015$), whereas no significant correlations were observed between MoCA scores and either part I or part II (part I: $r = -0.15$, $p = 0.44$; part II: $r = -0.21$, $p = 0.27$).

Among individual gait parameters, velocity, step length, and turning step width were correlated with MMSE (uncorrected $p < 0.05$, Table S4), but these correlations were not significant after correction. No significant correlations were found between MoCA scores and individual gait parameters (Fig. 3c).

Neurogenic OH (nOH) was identified in 24 patients (57.1%). Reduction in systolic and diastolic blood pressure upon standing were not significantly correlated with MSA-C gait pattern scores (sBP: $r = 0.32$, $p = 0.27$; dBP: $r = 0.25$, $p = 0.27$). Although the mean MSA-C gait pattern score was higher in patients with nOH compared to those without (4.0 ± 2.0 vs. 3.5 ± 1.9), this difference was not statistically significant ($p = 0.39$) (Figure S5).

Structural connectivity and volumetric analysis

Correlation-based tractography analysis (threshold: $t > 2.5$) identified 791 tracts associated with MSA-C gait pattern scores (Fig. 4a). Of these, 80.7% ($n = 631$) were located in the middle cerebellar peduncle (MCP), while 17.6% ($n = 139$) were association fibers within the right cingulum connecting frontoparietal regions. FA values in these tracts were negatively correlated with MSA-C gait pattern score ($r = -0.54$, $p = 0.013$) (Fig. 4b).

A total of 352 tracts were associated with UMSAR part II scores and DTI, primarily within the MCP (95.1%, $n = 335$) and right cerebellum (4.8%, $n = 17$) (Fig. 4c). However, FA values in these tracts were not significantly correlated with the UMSAR part II scores ($r = -0.089$, $p = 0.68$) (Fig. 4d).

Whole-brain VBM analysis revealed significant negative correlations between MSA-C gait pattern score and gray matter volume in the left middle temporal region ($r = -0.71$, $p = 0.013$) (Fig. 4e, f). Additional correlations were observed in the right middle temporal region ($r = -0.69$, $p = 1.8 \times 10^{-4}$) and left cerebellum ($r = -0.67$, $p = 0.0030$) (Figure S6). No significant correlations were observed between gray matter volume and UMSAR part I and II scores.

Discussion

This study demonstrates that a comprehensive motor pattern, extracted from 2D gait videos, robustly distinguishes patients with MSA-C. The MSA-C gait pattern not only reflects on motor severity—as evidenced by strong correlations with UMSAR part I and II scores—but also captures cognitive function and structural brain changes implicated in MSA-C. These findings suggest that the MSA-C gait pattern score may serve as a biomarker reflecting both clinical and pathophysiological features of the disease.

Motor aspects of the MSA-C gait pattern score

The MSA-C gait pattern score was significantly associated with UMSAR scores, particularly items related to gait, axial, and limb function of the part II, underscoring its relevance to core motor impairments in MSA-C. In contrast, tremor, which is a less prominent and prognostically relevant marker in MSA-C, showed weaker correlations, consistent with previous findings[10,18].

Although prior studies have shown correlations between UMSAR scores and disease duration[10], neither UMSAR scores nor MSA-C gait pattern score correlated significantly with disease duration in our cohort. This is likely due to the relatively early stage of disease in our sample (mean disease duration = 1.8 years).

Importantly, our gait scores integrated features from both locomotion (step length, step width, and velocity) and turning (turning step length and velocity). Previous studies have examined these aspects separately in MSA-C[17,19]. However, our study combines them into a composite biomarker. A recent study also emphasized turning metrics extracted from video are associated with postural instability[17]. Given the strong clinical relevance of gait, falls, turning, and axial symptoms in MSA-C progression[7], the MSA-C gait pattern score may serve a useful tool for monitoring MSA-C disease evolution.

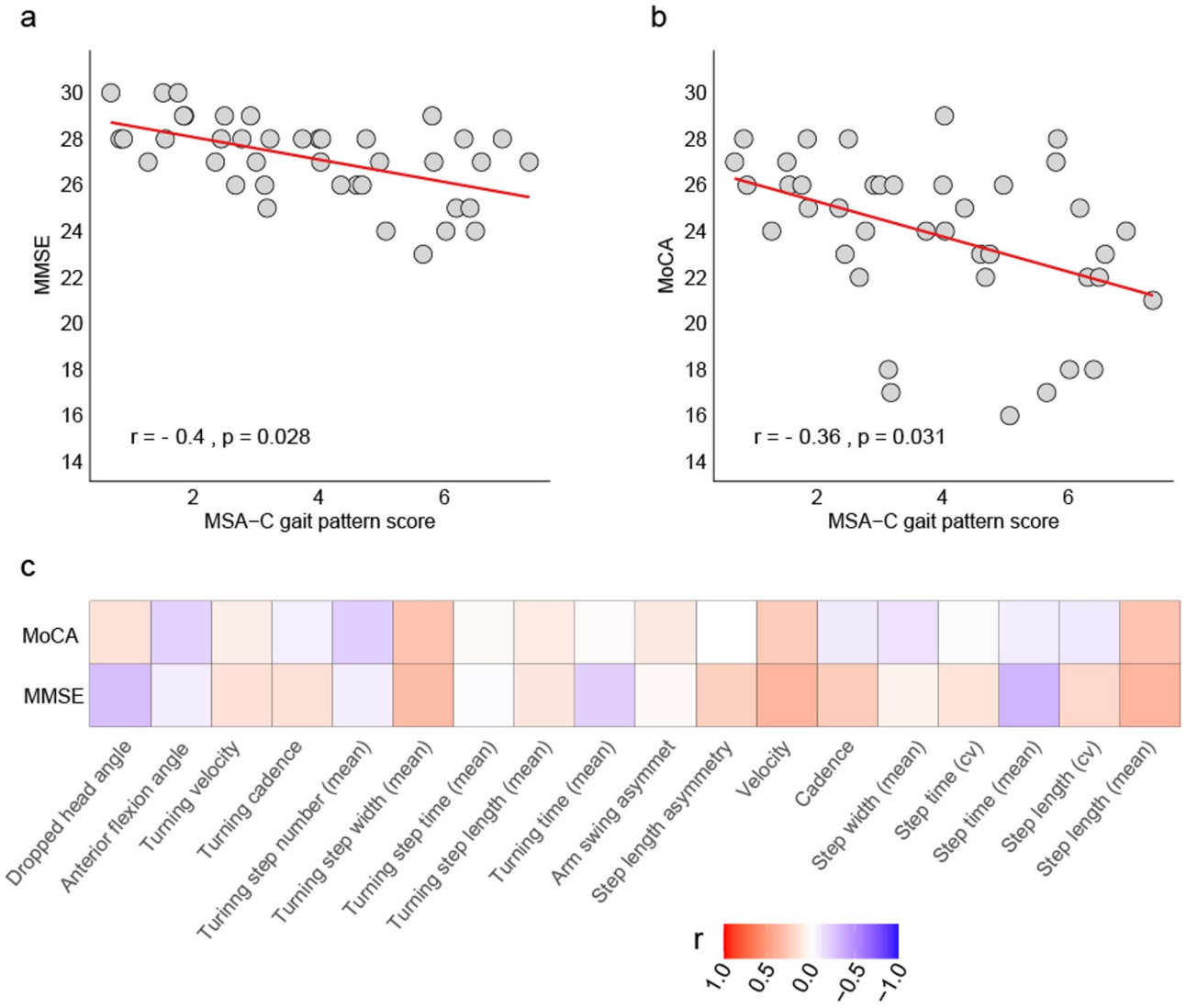

Fig. 3. Correlation between two cognitive profiles and the MSA-C gait pattern score, as well as its subscores. Scatter plots illustrate the correlations: (**a**) MSA-C gait pattern score and MMSE, (**b**) MSA-C gait pattern score and MoCA, (**c**) 18 gait parameters and MoCA, and MMSE. In each cell, colors indicate the strength of the Spearman partial correlation coefficients, adjusted for age, sex, and disease duration. Statistical significance was denoted with an asterisk (*). *$p < 0.05$, **$p < 0.01$, ***$p < 0.001$. Units: degree—anterior flexion angle, dropped head angle; meter—step length (mean), turning step length (mean), turning step width (mean); meter/second—velocity; second—step time (mean), turning step time (mean); steps per minute—cadence, turning cadence; meter—step length (mean), turning step length (mean), turning step width (mean); meter/second—velocity; second—step time (mean), turning step time (mean); steps per minute—cadence, turning cadence. *MMSE* Mini-Mental State Examination, *MoCA* Montreal Cognitive Assessment, *MSA-C* Multiple System Atrophy-Cerebellar type, *UMSAR* Unified Multiple System Atrophy Rating.

Non-motor aspects of the MSA-C gait pattern score

Cognitive dysfunction in MSA is primarily characterized by deficits in executive functions, including attention and working memory[20]. Additional impairments in memory and visuospatial function have also been reported[21,22], and global cognitive decline is reflected by reduced MMSE scores[21]. MSA-C group has been reported to have more impairments in attention[23,24], executive function[24,25], and verbal fluency[25], although the findings have been inconsistent across studies[26].

Gait is a complex motor behavior involving multiple levels of neural control from spinal circuits to cortical levels, requiring dynamic integration of motor control, sensory input, and cognitive processes. While cerebellar ataxic gait, a hallmark of MSA-C, has traditionally been categorized as a middle-level gait disorder[27], cognitive dysfunction—particularly in impaired motor planning and execution—may contribute to higher-level gait abnormalities[28,29]. This view is supported by study in other conditions. For example, in mild cognitive impairment, gait impairments (e.g., slower gait speed and reduced step length) are associated with dysfunctions in processing speed, executive function, and working memory[30,32]. Similarly, executive dysfunction and attentional deficits

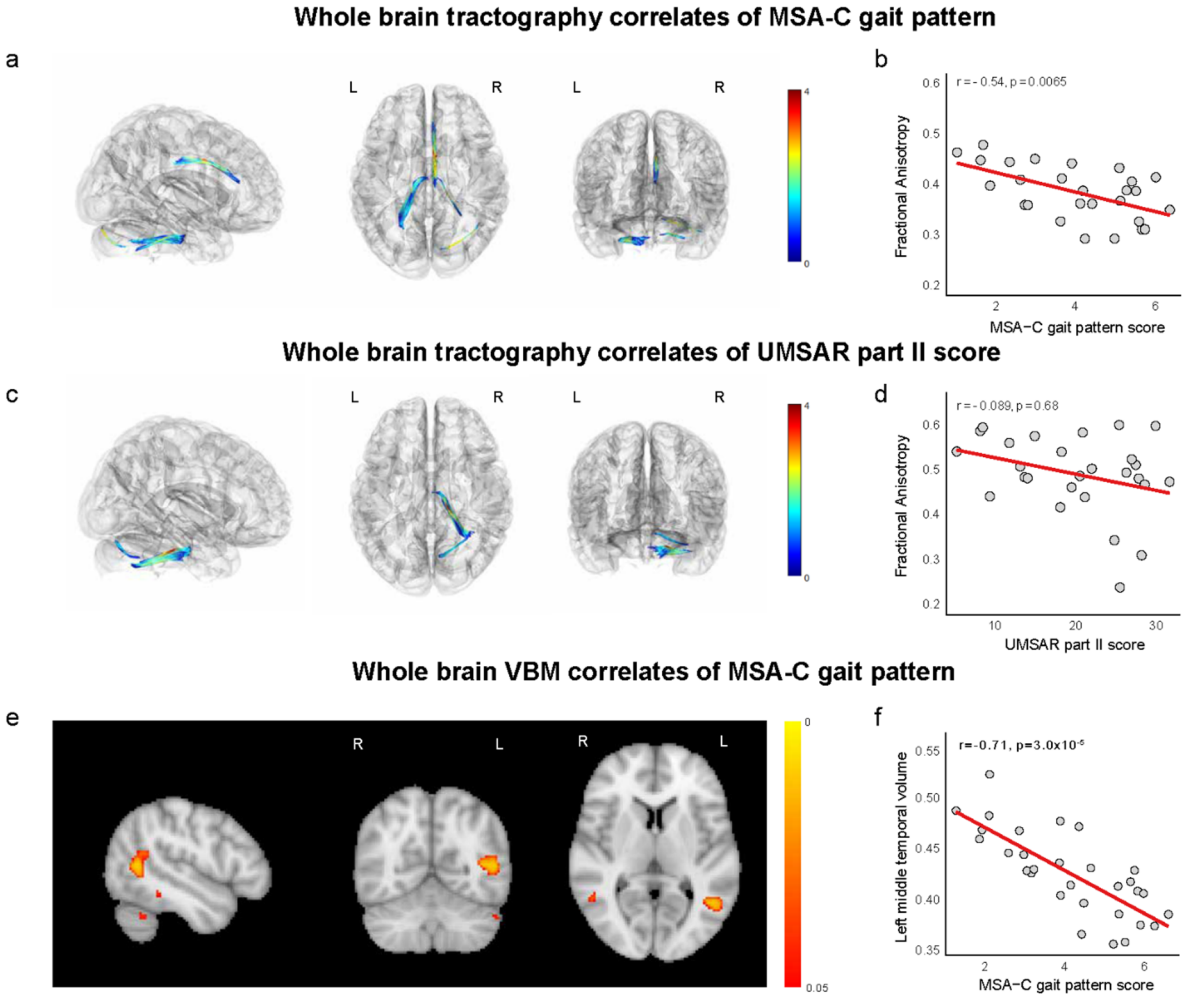

Fig. 4. Results of VBM and correlation tractography showing associations between brain structure and clinical parameters. (**a**) Neural correlates of the MSA-C gait pattern score. (**b**) Scattered plot between FA and the MSA-C gait pattern score. (**c**) Neural correlates of the UMSAR part II score. The color bars in (**a,c**) denote t-statistics. (**d**) Scatter plot between FA and the UMSAR part II score. (**e**) VBM correlates of the MSA-C gait pattern score. The color bar denotes family-wise error rate corrected p-value. (**f**) Scatter plot between left middle frontal area volume and the MSA-C gait pattern score. All correlations shown are Spearman partial correlations adjusted for age, sex, and disease duration. *FA* fractional anisotropy, *MSA-C* Multiple System Atrophy-Cerebellar type, *UMSAR* Unified Multiple System Atrophy Rating, *VBM* voxel-based volumetry.

have been associated with slower gait speed, increased stride-time variability, and impaired turning in patients with PD, highlighting the involvement of higher-level cognitive processes beyond motor symptoms[33]. The attention and executive dysfunction domains are linked to increased stride variability and slower gait during dual-task walking, which may require compensatory recruitment of prefrontal regions[34].

In our cohort, most patients had preserved or only mildly impaired cognition (MMSE ≥ 26 in 82.5%; MoCA scores ≥ 23 in 72.5%)[35,36]. Despite this, significant negative correlations between the MSA-C gait pattern score and both MMSE and MoCA scores indicate that even mild cognitive deficits may contribute to gait abnormalities. Interestingly, UMSAR part II correlated only with MMSE but not with MoCA. Given that MoCA is more sensitive to executive and attention deficits[37], this may reflect the greater involvement of these domains in MSA-C.

Previous studies have linked UMSAR scores to cognitive domains such as mental flexibility and response inhibition[38–40], but few have examined the relationship between cognition and gait. Our findings support the hypothesis that even mild frontal-executive and attentional dysfunction contributes to gait abnormalities in MSA-C and is reflected in the MSA-C gait pattern score.

MSA-C gait pattern scores did not differ between patients with and without neurogenic orthostatic hypotension (nOH), nor were they correlated with orthostatic blood pressure changes. Although previous studies report association between nOH and disease severity, including the UMSAR part II score[41], the lack of association in our study may be due to early stage of disease in our cohort, warranting longitudinal follow-up.

Structural connectivity and volumetric analysis

Extensive structural changes in both gray and white matter have been in MSA-C, especially in the sensorimotor regions and white matter tracts of the cerebellum, brainstem, and corticospinal pathway[42,43]. FA reductions in the MCP are strongly correlated with motor severity, highlighting its role as a key determinant of motor function in MSA-C[44]. In our study, both the MSA-C gait pattern score and UMSAR part II score correlated with MCP, supporting previous findings[44].

However, several key differences emerged. First, volumetric correlation in the cerebellum was significant only for the MSA-C gait score. Additionally, the extent and statistical significance of fiber tract correlations in the MCP were greater for the MSA-C gait score than in for the UMSAR part II score. (Fig. 4c, d). The absence of significant cerebellar tract correlations with the UMSAR part II score (Fig. 4d) may be due to weaker associations between parameters and the tract. These findings suggest that the MSA-C gait pattern score may more accurately reflect cerebellar and MCP involvement—key structures implicated in motor dysfunction in MSA-C—than the conventional UMSAR part II score.

Beyond the cerebellum, the MSA-C gait pattern score exhibited broader structural correlations in supratentorial area, including reduced volume in the middle temporal gyrus and decreased neural tract integrity in the cingulate gyrus—findings not observed with the UMSAR part II score.

Alterations in the cingulate gyrus have been implicated in MSA-C, with studies linking them to motor and gait disturbances. Patients with MSA-C show reduced FA in the cingulate compared to HCs. Given its well-established role in attentional processing and executive control, cingulate dysfunction has also been associated with impaired sustained attention and attentional regulation in psychiatric conditions[45–47]. Functional MRI studies have shown reduced motor-related activation in the anterior cingulate cortex following levodopa administration in MSA patients, suggesting impaired motor integration[48]. Moreover, patients with MSA-C and freezing of gait exhibit decreased functional connectivity in the left anterior cingulate cortex, highlighting its role in higher-order motor control[49]. Together, these findings support the idea that cingulate dysfunction contributes to both cognitive and motor impairments in MSA-C.

In line with our observation showing significant volumetric correlations in the VBM analysis, the MTG has been shown to undergo atrophy in MSA, particularly in patients with mild cognitive impairment[50,51]. Moreover, reduced MTG thickness has also been associated with longer disease duration and greater cognitive decline[51].

Taken together, our findings suggest that the MSA-C gait pattern score reflects not only cerebellar abnormalities, but also supratentorial changes in regions involved in cognitive and higher-order motor control. In contrast, no significant structural or volumetric associations were observed for the UMSAR part II scores. These results underscore the potential utility of the video-based MSA-C gait score as a more sensitive marker of the pathophysiological burden in MSA-C, integrating both motor and cognitive domains.

Our findings suggest that the video-based MSA-C gait pattern could be translated from a research tool into a practical instrument. Because it can be derived from a single 2D video, this approach is feasible with simple devices such as smartphones, this approach also lends itself to home-based application[14,16,17], thereby improving accessibility and scalability. This approach may provide a means of estimating clinical severity directly from simple repetitive gait recordings, without the need for a separate interview or detailed examination. Integration with other modalities, including fluid biomarkers, may further enhance diagnostic accuracy and prognostic precision[52]. It has also been reported that patients with idiopathic REM sleep behavior disorder exhibit subtle gait changes[53], and that gait differences can be observed between MSA-P and PD[54]. Applying our approach to patients with early or prodromal stage and comparing across related disorders could therefore provide additional information and could improve differential diagnostic accuracy. Together, these features underscore the added value of this biomarker for real-world monitoring and clinical utility in MSA-C.

This study has several limitations. First, the sample size was relatively small, and the study was conducted at a single center without an independent validation cohort, which may limit the generalizability of the findings. Furthermore, although we present the video-based gait score as a digital biomarker[55,56], it has not yet been validated for reproducibility across independent cohorts or recording conditions, nor has it been directly compared with other parkinsonian or ataxia syndromes. These limitations warrant further investigation to confirm its robustness and clinical applicability. Nevertheless, given the rarity of MSA-C and the limited availability of datasets combining video-based analyses with neuroimaging, our study offers valuable insights into the clinical and pathophysiology correlates of gait dysfunction in MSA-C. Second, this was a cross-sectional study, which limits our ability to assess longitudinal changes in gait patterns and their relationship with disease progression. Also, our findings indicate correlations rather than causal relationships between cognitive dysfunction and gait impairments. Third, we did not include a comprehensive neuropsychological battery to evaluate specific cognitive domains. As a result, our ability to delineate domain-specific cognitive correlates of gait abnormalities was limited. Moreover, in the control group, cognitive status was initially assessed through interview-based screening rather than formal cognitive testing, and thus not all evaluations were available. Fourth, while our tractography findings were located far from the frontotemporal areas prone to susceptibility artifacts, we could not perform artifact correction using an opposite phase-encoding image, which may have affected the results. Lastly, our MSA-C cohort consisted of primarily individuals in the early stage of the disease, which may limit the generalizability of our findings.

In conclusion, our study demonstrates that gait patterns extracted from a single 2D video camera are associated with both motor and cognitive features in patients with MSA-C. The MSA-C gait pattern scores showed strong correlations with clinical severity and neuroanatomical changes. These findings suggest that the gait pattern scores may serve as markers of disease severity with MSA-C. Longitudinal studies with larger and more diverse cohorts are needed to validate the potential utility of this approach in tracking disease progression.

Methods

Patient enrollment

This cross-sectional study included patients with MSA-C and healthy controls (HCs) recruited between January 2019 and August 2024 at the Movement Disorder Clinic of Seoul National University Hospital. MSA-C was diagnosed by movement disorder experts (J.H.S. and H.J.K.) based on the 2022 Movement Disorder Society MSA diagnostic criteria[7]. Patients fulfilling the diagnostic criteria for probable or established MSA-C and with a disease duration of no more than five years were included. Exclusion criteria included any history of neurological diseases other than MSA-C, musculoskeletal or spinal disorders that could affect gait or posture. In addition, HCs were required to show no cognitive abnormalities during the screening interview or to have an MMSE score greater than 24. A comprehensive examination was conducted for patients with MSA-C, including the UMSAR, Mini Mental State Examination (MMSE), Montreal Cognitive Assessment (MoCA), and orthostatic hypotension (OH) test. Brain magnetic resonance imaging (MRI) was performed during the same clinical visit.

The study protocol was approved by the Institutional Review Board (IRB) of Seoul National University Hospital (IRB Nos. 0703-044-201 and 2404-043-1526). Written informed consent was obtained from all participants before enrollment, and the study was conducted in accordance with the Declaration of Helsinki. In addition, written informed consent for publication of identifying information/images in an online open-access publication was obtained from all participants.

Gait video acquisition and pattern generation

All participants were instructed to walk, completing at least two round trips along a 7-meter walkway while repeating the following sequence: walking 7 m forward, turning around (180 °), walking 7 m back to the starting point, and turning around again (180°). The videos were recorded from the front view while walking. The starting and turning points for each task were marked by a horizontal line on the floor (Fig. 1a). Recordings were made using a camera (PXW-Z190V; SONY, Japan) mounted on a tripod positioned 1.5 m from the horizontal line marking the turning point.

We used a quantitative gait analysis algorithm (Gaitome)[14,17] used in our previous study. The extracted parameters consisted of 18 gait parameters, including eight forward gait parameters (step length, step time, step width, step length variability, step time variability, cadence, and velocity), two asymmetry measures (arm swing asymmetry and step length asymmetry), seven turning-related parameters (turning time, turning step length, turning step time, turning step base, turning step number, turning cadence, and turning velocity), and two posture parameters (anterior flexion angle and dropped head angle).

Disease-related gait pattern scores were generated using a scaled subprofile model of the principal component analysis (SSM-PCA) method[57] using custom-written code with MATLAB 2022b (MathWorks, Natick, MA). From the 18 gait parameters matrix obtained from HCs and age- and sex-matched patients with MSA-C, we extracted a shared covariance structure (Fig. 1b, c) that reflects the common gait variance across both groups. SSM-PCA identified component patterns that captured deviations from this normative structure, thereby emphasizing disease-specific gait alterations. Subsequently, we designed multiple linear regression models using every combination of the first five principal components (PCs) as independent variables and group (MSA-C versus HCs) as the dependent variable. We computed the area under the curve (AUC) in models with every combination of PCs to differentiate patients with MSA-C from HCs. The model with the highest AUC was designated as the MSA-C pattern. The MSA-C gait pattern scores were calculated for each participant and subsequently normalized using a generalized linear model (GLM) fitted to a healthy control group, with age, sex, and height as predictors. To validate the stable regions among the gait related parameters, the weights of each parameter of patients and HCs were boot-strap resampled 1000 times. This approach was used to define a normative reference independent of disease-related variations.

MRI data acquisition

All MR images were acquired using a 3.0 T MR scanner (Ingenia CX, Philips Healthcare, Best, Netherlands) with a conventional head-gradient coil. T1-weighted imaging and diffusion tensor imaging (DTI) were acquired with the following scan parameters: (1) 3D high-resolution magnetization prepared rapid gradient echo (MPRAGE) T1-weighted sequence (TR = 1600 ms, TE = 2.8 ms, inversion time = 900 ms, flip angle = 12°, FOV = 220 mm, matrix = 225 × 225, slice thickness = 1 mm, no gap, and voxel size = 1 × 1 × 1 mm) and (2) spin-echo single-shot echo-planar imaging diffusion-weighted sequence (TR = 4400 ms, TE = 75 ms, number of excitations = 1, matrix = 112 × 112, FOV = 224 × 224 mm, number of slices = 75, slice thickness = 2 mm, slice gap = 0 mm, orientation = axial, b = 1000 s/mm2 and one additional b0-volume). We used 64 nonlinear diffusion-weighting gradient directions to estimate the intensity and direction of diffusion anisotropy. Among the 30 patients with brain MRI, DTI analysis was available for 27, whereas all underwent VBM analysis.

Voxel-based morphometric analysis

Voxel-based morphometry was analyzed using FSL-VBM[58]. Briefly, structural images were extracted from the brain and gray matter was segmented to create a study-specific gray matter template. All native grey matter images were nonlinearly registered to this study-specific template and modulated to correct for local expansion or contraction. The modulated gray matter images were then smoothed using a Gaussian kernel with a sigma of 3 mm. The output of each analysis stage was visually checked according to the FSL-VBM guidelines. Finally, a voxel-wise GLM was applied to determine whether gray matter volume correlated with the MSA-C gait pattern score. Threshold-free cluster enhancement (TFCE)[59] was used to account for multiple comparisons by controlling for family wise error (FWE) rate at $p < 0.05$. Total intracranial volume, age, sex, and disease duration were used as covariates in the analysis.

Diffusion MRI correlational tractography

Correlational tractography was used to explore the local connectome associated with the MSA-C gait pattern score. Subsequent analyses were performed using DSI Studio (http://dsi-studio.labsolver.org)[60]. DTI preprocessing included noise correction using MRtrix3[61] and eddy current correction using FSL Eddy[62]. For quality control, DSI Studio performed an outlier check, labeling images as a 'low-quality outlier' if the correlation coefficient was > 3 standard deviation from the absolute mean. None of our scans were flagged as outliers[63]. The b-table quality control, motion, and eddy current corrections were performed using the built-in preprocessing routine of DSI Studio. Corrected data were reconstructed in the MNI space using Q-Space Diffeomorphic Reconstruction (QSDR)[64]. The core hypothesis in correlation tractography is that associations between local connectomes and study variables propagate along a common fiber pathway. This hypothesis can be tested by tracking local connectomes that show substantial association with clinical scores into a "track." The length of this track is then compared to a null distribution created by a permutation test. Specifically, as described in the original paper[60], the tracking algorithm used a total of 10 seeds per local connectome within its voxel to initiate tracking. This procedure was performed for a set of 5,000 local connectome matrices obtained through bootstrapping resampling. Fractional anisotropy (FA), generally interpreted as a quantitative biomarker of white matter "integrity," was used in the correlational tractography analysis[65]. A non-parametric Spearman partial correlation was used to derive the correlation, and the effects of age and sex were removed using a multiple regression model. To map the different levels of correlation, we selected t-score thresholds of 2.5[63]. The tracks were filtered by topology-informed pruning with a length threshold of 20 voxel distances used to select tracks[65,66]. A total of 4000 randomized permutations were applied to control the false discovery rate (FDR) < 0.05.

Statistical analysis

Normality of the data was assessed using the Q-Q plot and Shapiro-Wilk test, and homogeneity of variances was evaluated using Levene's test. Correlation analyses between gait pattern features and clinical parameters were conducted using Spearman's partial correlation tests with age, height, and disease duration as covariates. Differences between two groups were evaluated using the t-test or Wilcoxon rank-sum test. Differences in categorical variables were assessed using the chi-square test. A two-tailed p-value of less than 0.05 was considered statistically significant. All regional p-values are corrected with the Benjamini–Hochberg (BH) FDR method. Statistical analyses were performed using the R version 4.4.2 (https://www.r-project.org/) and MATLAB 2022b (MathWorks, Natick, MA, USA).

Data availability

The raw data supporting the findings of the present study are available on request from the corresponding author.

Received: 1 August 2025; Accepted: 28 October 2025
Published online: 15 December 2025

References

1. Stankovic, I., Fanciulli, A., Sidoroff, V. & Wenning, G. K. A review on the clinical diagnosis of multiple system atrophy. *Cerebellum* **22**, 825–839 (2023).
2. Zhang, L. et al. Prediction of early-wheelchair dependence in multiple system atrophy based on machine learning algorithm: A prospective cohort study. *Clin. Park Relat. Disord.* **8**, 100183 (2023).
3. Foubert-Samier, A. et al. Disease progression and prognostic factors in multiple system atrophy: A prospective cohort study. *Neurobiol. Dis.* **139**, 104813 (2020).
4. Low, P. A. et al. Natural history of multiple system atrophy in the USA: a prospective cohort study. *Lancet Neurol.* **14**, 710–719 (2015).
5. Kim, H. J., Jeon, B. S., Lee, J. Y. & Yun, J. Y. Survival of Korean patients with multiple system atrophy. *Mov. Disord.* **26**, 909–912 (2011).
6. Bendetowicz, D. et al. Recent advances in clinical trials in multiple system atrophy. *Curr. Neurol. Neurosci. Rep.* **24**, 95–112 (2024).
7. Wenning, G. K. et al. The movement disorder society criteria for the diagnosis of multiple system atrophy. *Mov. Disord.* **37**, 1131–1148 (2022).
8. Levin, J. et al. Safety and efficacy of Epigallocatechin gallate in multiple system atrophy (PROMESA): a randomised, double-blind, placebo-controlled trial. *Lancet Neurol.* **18**, 724–735 (2019).
9. Palma, J. A. et al. Limitations of the unified multiple system atrophy rating scale as outcome measure for clinical trials and a roadmap for improvement. *Clin. Auton. Res.* **31**, 157–164 (2021).
10. Krismer, F. et al. The unified multiple system atrophy rating scale: Status, Critique, and recommendations. *Mov. Disord.* **37**, 2336–2341 (2022).
11. Lee, S. W. & Koh, S. B. Clinical features and disability milestones in multiple system atrophy and progressive supranuclear palsy. *J. Mov. Disord.* **5**, 42–47 (2012).
12. Tang, W., van Ooijen, P. M. A., Sival, D. A. & Maurits, N. M. Automatic two-dimensional & three-dimensional video analysis with deep learning for movement disorders: A systematic review. *Artif. Intell. Med.* **156**, 102952 (2024).
13. Novotny, M. et al. Automated video-based assessment of facial bradykinesia in de-novo parkinson's disease. *NPJ Digit. Med.* **5**, 98 (2022).
14. Shin, J. H. et al. Quantitative gait analysis using a Pose-Estimation algorithm with a single 2D-Video of parkinson's disease patients. *J. Parkinsons Dis.* **11**, 1271–1283 (2021).
15. Deng, D. et al. Interpretable video-based tracking and quantification of parkinsonism clinical motor States. *NPJ Parkinsons Dis.* **10**, 122 (2024).
16. Shin, J. H. et al. Objective measurement of limb bradykinesia using a marker-less tracking algorithm with 2D-video in PD patients. *Parkinsonism Relat. Disord.* **81**, 129–135 (2020).
17. Jeon, H. et al. Spatiotemporal gait parameters during turning and imbalance in parkinson's disease: Video-Based analysis from a single camera. *J. Mov. Disord.* **18**, 87–92 (2025).
18. Zhang, L. et al. Longitudinal evolution of motor and non-motor symptoms in early-stage multiple system atrophy: a 2-year prospective cohort study. *BMC Med.* **20**, 446 (2022).

19. Schniepp, R., Mohwald, K. & Wuehr, M. Key gait findings for diagnosing three syndromic categories of dynamic instability in patients with balance disorders. *J. Neurol.* **267**, 301–308 (2020).
20. Stankovic, I. et al. Cognitive impairment in multiple system atrophy: a position statement by the neuropsychology task force of the MDS multiple system atrophy (MODIMSA) study group. *Mov. Disord.* **29**, 857–867 (2014).
21. Brown, R. G. et al. Cognitive impairment in patients with multiple system atrophy and progressive supranuclear palsy. *Brain* **133**, 2382–2393 (2010).
22. Lyoo, C. H. et al. Effects of disease duration on the clinical features and brain glucose metabolism in patients with mixed type multiple system atrophy. *Brain* **131**, 438–446 (2008).
23. Barcelos, L. B. et al. Neuropsychological and clinical heterogeneity of cognitive impairment in patients with multiple system atrophy. *Clin. Neurol. Neurosurg.* **164**, 121–126 (2018).
24. Eschlbock, S. et al. Cognition in multiple system atrophy: a single-center cohort study. *Ann. Clin. Transl Neurol.* **7**, 219–228 (2020).
25. Chang, C. C. et al. Cognitive deficits in multiple system atrophy correlate with frontal atrophy and disease duration. *Eur. J. Neurol.* **16**, 1144–1150 (2009).
26. Kim, H. J. et al. Clinical and imaging characteristics of dementia in multiple system atrophy. *Parkinsonism Relat. Disord.* **19**, 617–621 (2013).
27. Nutt, J. G., Marsden, C. D. & Thompson, P. D. Human walking and higher-level gait disorders, particularly in the elderly. *Neurology* **43**, 268–279 (1993).
28. Takakusaki, K. Functional neuroanatomy for posture and gait control. *J. Mov. Disord.* **10**, 1–17 (2017).
29. Nutt, J. G. Higher-level gait disorders: an open frontier. *Mov. Disord.* **28**, 1560–1565 (2013).
30. Doi, T. et al. Cognitive function and gait speed under normal and dual-task walking among older adults with mild cognitive impairment. *BMC Neurol.* **14**, 67 (2014).
31. Muurling, M. et al. Gait disturbances are associated with increased cognitive impairment and cerebrospinal fluid Tau levels in a memory clinic cohort. *J. Alzheimers Dis.* **76**, 1061–1070 (2020).
32. Taniguchi, Y., Yoshida, H., Fujiwara, Y., Motohashi, Y. & Shinkai, S. A prospective study of gait performance and subsequent cognitive decline in a general population of older Japanese. *J. Gerontol. Biol. Sci. Med. Sci.* **67**, 796–803 (2012).
33. Amboni, M., Barone, P. & Hausdorff, J. M. Cognitive contributions to gait and falls: evidence and implications. *Mov. Disord.* **28**, 1520–1533 (2013).
34. Kang, S. H., Kim, J., Lee, J. & Koh, S. B. Mild cognitive impairment is associated with poor gait performance in patients with parkinson's disease. *Front. Aging Neurosci.* **14**, 1003595 (2022).
35. Carson, N., Leach, L. & Murphy, K. J. A re-examination of Montreal cognitive assessment (MoCA) cutoff scores. *Int. J. Geriatr. Psychiatry.* **33**, 379–388 (2018).
36. Thomann, A. E., Berres, M., Goettel, N., Steiner, L. A. & Monsch, A. U. Enhanced diagnostic accuracy for neurocognitive disorders: a revised cut-off approach for the Montreal cognitive assessment. *Alzheimers Res. Ther.* **12**, 39 (2020).
37. Marinus, J., Verbaan, D. & van Hilten, J. J. The MoCA: well-suited screen for cognitive impairment in Parkinson disease. *Neurology* **76**, 1944–1945 (1944).
38. Dash, S. et al. Cognition in patients with multiple system atrophy (MSA) and its neuroimaging correlation: A prospective case-control study. *Cureus* **14**, e21717 (2022).
39. Hatakeyama, M. et al. Predictors of cognitive impairment in multiple system atrophy. *J. Neurol. Sci.* **388**, 128–132 (2018).
40. Li, N. et al. A study on the characteristics of cognitive function in patients with multiple system atrophy in China. *Sci. Rep.* **11**, 4995 (2021).
41. Jiang, Q. et al. Orthostatic hypotension in multiple system atrophy: related factors and disease prognosis. *J. Parkinsons Dis.* **13**, 1313–1320 (2023).
42. Faber, J. et al. Prominent white matter involvement in multiple system atrophy of cerebellar type. *Mov. Disord.* **35**, 816–824 (2020).
43. Raghavan, S. et al. White matter abnormalities track disease progression in multiple system atrophy. *Mov. Disord Clin. Pract.* **11**, 1085–1094 (2024).
44. Lin, D. J., Hermann, K. L. & Schmahmann, J. D. The diagnosis and natural history of multiple system Atrophy, cerebellar type. *Cerebellum* **15**, 663–679 (2016).
45. Wu, D. et al. Persistent neuronal activity in anterior cingulate cortex correlates with sustained attention in rats regardless of sensory modality. *Sci. Rep.* **7**, 43101 (2017).
46. Bush, G. et al. Anterior cingulate cortex dysfunction in attention-deficit/hyperactivity disorder revealed by fMRI and the counting Stroop. *Biol. Psychiatry.* **45**, 1542–1552 (1999).
47. Dash, S. K. et al. Abnormalities of white and grey matter in early multiple system atrophy: comparison of parkinsonian and cerebellar variants. *Eur. Radiol.* **29**, 716–724 (2019).
48. Payoux, P. et al. Motor activation in multiple system atrophy and Parkinson disease: a PET study. *Neurology* **75**, 1174–1180 (2010).
49. Cheng, Y., Yang, H., Liu, W. V., Wen, Z. & Chen, J. Alterations of brain activity in multiple system atrophy patients with freezing of gait: A resting-state fMRI study. *Front. Neurosci.* **16**, 954332 (2022).
50. Lin, J., Xu, X., Hou, Y., Yang, J. & Shang, H. Voxel-Based Meta-Analysis of Gray matter abnormalities in multiple system atrophy. *Front. Aging Neurosci.* **12**, 591666 (2020).
51. Cao, C. et al. Morphological changes in cortical and subcortical structures in multiple system atrophy patients with mild cognitive impairment. *Front. Hum. Neurosci.* **15**, 649051 (2021).
52. Brzenczek, C. et al. Integrating digital gait data with metabolomics and clinical data to predict outcomes in parkinson's disease. *NPJ Digit. Med.* **7**, 235 (2024).
53. McDade, E. M. et al. Subtle gait changes in patients with REM sleep behavior disorder. *Mov. Disord.* **28**, 1847–1853 (2013).
54. Na, B. S. et al. Comparison of gait parameters between drug-naive patients diagnosed with multiple system atrophy with predominant parkinsonism and parkinson's disease. *Parkinsonism Relat. Disord.* **60**, 87–91 (2019).
55. Califf, R. M. Biomarker definitions and their applications. *Exp. Biol. Med. (Maywood).* **243**, 213–221 (2018).
56. Macias Alonso, A. K., Hirt, J., Woelfle, T., Janiaud, P. & Hemkens, L. G. Definitions of digital biomarkers: a systematic mapping of the biomedical literature. *BMJ Health Care Inform.* **31** (2024).
57. Spetsieris, P. G. & Eidelberg, D. Scaled subprofile modeling of resting state imaging data in parkinson's disease: methodological issues. *Neuroimage* **54**, 2899–2914 (2011).
58. Douaud, G. et al. Anatomically related grey and white matter abnormalities in adolescent-onset schizophrenia. *Brain* **130**, 2375–2386 (2007).
59. Smith, S. M. & Nichols, T. E. Threshold-free cluster enhancement: addressing problems of smoothing, threshold dependence and localisation in cluster inference. *Neuroimage* **44**, 83–98 (2009).
60. Yeh, F. C., Badre, D., Verstynen, T. & Connectometry A statistical approach Harnessing the analytical potential of the local connectome. *Neuroimage* **125**, 162–171 (2016).
61. Veraart, J. et al. Denoising of diffusion MRI using random matrix theory. *Neuroimage* **142**, 394–406 (2016).
62. Andersson, J. L. R., Graham, M. S., Drobnjak, I., Zhang, H. & Campbell, J. Susceptibility-induced distortion that varies due to motion: correction in diffusion MR without acquiring additional data. *Neuroimage* **171**, 277–295 (2018).
63. Pritschet, L. et al. Neuroanatomical changes observed over the course of a human pregnancy. *Nat. Neurosci.* **27**, 2253–2260 (2024).
64. Yeh, F. C., Wedeen, V. J. & Tseng, W. Y. Estimation of fiber orientation and spin density distribution by diffusion Deconvolution. *Neuroimage* **55**, 1054–1062 (2011).

65. Kim, M. et al. Structural Disconnection is associated with disability in the neuromyelitis Optica spectrum disorder. *Brain Imaging Behav.* **17**, 664–673 (2023).
66. Mosch, B., Hagena, V., Herpertz, S. & Diers, M. Brain morphometric changes in fibromyalgia and the impact of psychometric and clinical factors: a volumetric and diffusion-tensor imaging study. *Arthritis Res. Ther.* **25**, 81 (2023).

Acknowledgements
This work was supported by the National Research Foundation (NRF) grants funded by Ministry of Science and ICT (NRF-2021R1C1C1011077) and by the Ministry of Education (RS-2023-00262880) in South Korea.

Author contributions
Seungmin Lee contributed to the conception and design of the study, acquisition and interpretation of data, and drafting of the manuscript. Minchul Kim contributed to data acquisition and analysis, drafting of the manuscript. Kyu Sung Choi contributed to data acquisition and analysis, drafting of the manuscript. Chanhee Jeong contributed to the acquisition and interpretation of data, and drafting of the manuscript. Ri Yu contributed to the creation of new software used in the study and drafting of the manuscript. Jee-Young Lee contributed to data interpretation and drafting of the manuscript. Jung Hwan Shin contributed to the conception and design of the study, data acquisition and interpretation, and drafting of the manuscript. Han-Joon Kim contributed to data interpretation and drafting of the manuscript. Beomseok Jeon contributed to data interpretation and drafting of the manuscript. All authors have approved the submitted version of the manuscript and agree to be accountable for all aspects of the work.

Declarations

Competing interests
The authors declare no competing interests.

Additional information
Supplementary Information The online version contains supplementary material available at https://doi.org/10.1038/s41598-025-26389-z.

Correspondence and requests for materials should be addressed to J.H.S. or H.-J.K.

Reprints and permissions information is available at www.nature.com/reprints.

Publisher's note Springer Nature remains neutral with regard to jurisdictional claims in published maps and institutional affiliations.